Array Resonances of Periodic WEC Arrays in Front of a Reflecting Wall

Grgur Tokić & Dick K.P. Yue
Department of Mechanical Engineering, Massachusetts Institute of Technology, Cambridge MA 02139
gtokic@mit.edu

Introduction

Harnessing wave reflections is a well known approach to increase energy extraction. In WEC arrays, an infinite vertical wall, such as a breakwater or a coastal cliff face, can play a role of a mirror. Recently, hydrodynamic studies of small WEC arrays (5 bodies) in a limited number of configurations in front of a reflecting wall [1, 2] showed that the energy extraction gain can be significant (a ∼600% increase).

In this study, we consider periodic WEC arrays consisting of a single infinite row of converters located in front of an ideal reflecting vertical wall. We focus on the maximum energy extraction performance, and elucidate the physical underpinnings of extreme performance. We apply multiple scattering simulations of linear wave-array interactions and theoretical analysis to achieve these goals.

Problem Formulation

We study the hydrodynamic and energetic response of a periodic row of WECs in water of uniform depth h in front of and parallel to an infinite vertical wall, figure 1. All WECs are truncated cylinders of radius $a/h = 0.3$ and draft $H/h = 0.2$, figure 1a. WECs are oscillating in heave only, and each is connected to a power take-off (PTO) device with extraction rate $\beta = \beta^*$. Here, $\beta^* = b(k_\mathrm{r})$ is the optimal PTO extraction rate, which is equal to the radiation damping b at the body resonant wavenumber k_r.

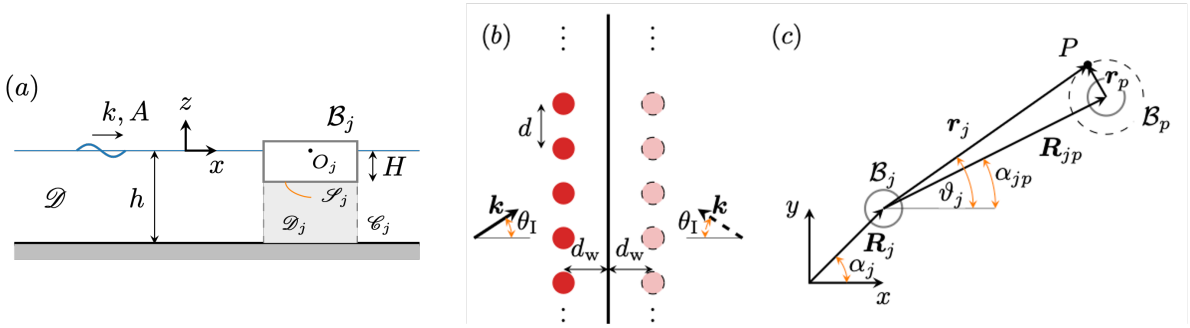

Figure 1: Spatial configurations of arrays. (a) Domain sketch. (b) C-W array (● = WEC; ● = mirrored (image) WEC). (c) Coordinate systems and position vector decomposition.

We primarily focus on the array gain $q = P/NP_0$, the ratio between the power P extracted by N converters in a periodic cell and the power P_0 that would be extracted by each of the N converters in isolation. This ratio quantifies the increase in energy extraction due to wave interactions between incident, reflected and radiated waves, and it is strongly dependent on the spatial array configuration.

Mathematical model

We consider linear waves (angular frequency ω, wavenumber k, amplitude A; $kA \ll 1$) and linear wave-body interactions under the potential flow assumption. The total complex potential $\phi = \phi^\mathrm{I} + \sum_{j=1}^{N} \left[\phi_j^\mathrm{S} + \phi_j^\mathrm{R}\right]$ of the flow around an array can be expressed as the sum of the ambient incident wave potential ϕ^I, and the scattered wave ϕ_j^S and radiated wave ϕ_j^R potentials of each body $\mathcal{B}_j$. (The time dependent real potential is $\Phi = \mathrm{Re}\left[\phi\, \mathrm{e}^{-\mathrm{i}\omega t}\right]$.)

Focusing on body $\mathcal{B}_p$, ϕ can be further rewritten in terms of ϕ_p^{S} and total incident wave potential ϕ_p^{I} on $\mathcal{B}_p$, where ϕ_p^{I} is the sum of the ambient incident wave on $\mathcal{B}_p$, and the scattered and radiated waves from all other bodies $\mathcal{B}_j$, $j \neq p$. In the cylindrical coordinate system (r_p, ϑ_p, z) centred at $\mathcal{B}_p$, figure 1c, these potentials can be expanded into partial waves as

$$\phi_p^{\mathrm{I}} = \sum_{m=0}^{\infty} \sum_{n=-\infty}^{\infty} d_{m,n}^{p} \mathrm{I}_n(k_m r_p) \mathrm{e}^{\mathrm{i}n\vartheta_p} \psi_m(z) \ , \quad \phi_p^{\mathrm{S}} = \sum_{m=0}^{\infty} \sum_{n=-\infty}^{\infty} c_{m,n}^{p} \mathrm{K}_n(k_m r_p) \mathrm{e}^{\mathrm{i}n\vartheta_p} \psi_m(z) \tag{1}$$

where $d_{m,n}^{p}$ and $c_{m,n}^{p}$ are the partial wave amplitudes. Here, I_n and K_n are the modified Bessel functions of the first and second kind, respectively, and ψ_m is the depth function; $k_0 \equiv -\mathrm{i}k$ corresponds to the propagating wave, $m > 0$ for evanescent waves. The incident wave amplitudes $d_{m,n}^{p}$ are the sum of the ambient incident wave $d_{m,n}^{\mathrm{I},p} = (-1)^n \exp\left[\mathrm{i}kR_p \cos(\theta_{\mathrm{I}} - \alpha_p) - \mathrm{i}n\theta_{\mathrm{I}}\right]$ at $\mathcal{B}_p$ and the contributions of the scattered and radiated waves $c_{m,n}^{j}$ of bodies $\mathcal{B}_j$ expressed in the $\mathcal{B}_p$ coordinate system. For notational convenience, we collect $d_{m,n}^{p}$ and $c_{m,n}^{p}$ into vectors $\boldsymbol{d}_p$ and $\boldsymbol{c}_p$, respectively; $\boldsymbol{d}_p^{\mathrm{I}}$ is the vector form of $d_{m,n}^{\mathrm{I},p}$.

The diffraction boundary condition $\partial(\phi_p^{\mathrm{I}} + \phi_p^{\mathrm{S}})/\partial n = 0$ on body $\mathcal{B}_p$ can then be expressed in terms of a linear system $\boldsymbol{c}_p = \mathbf{T}_p \cdot \boldsymbol{d}_p$ at each bodies $\mathcal{B}_p$, $p = 1, \ldots, N$, where $\mathbf{T}_p$ is the body-dependent scattering transfer matrix. Enforcing the boundary condition on every $\mathcal{B}_p$ in the arrays leads to a linear system for the unknown amplitudes $\boldsymbol{c}_p$, $p = 1, \ldots, N$

$$\sum_{j=1}^{N} \Big[\delta_{jp} - \mathbf{T}_j((1-\delta_{jp})\mathbf{S}_{jp} + \mathbf{Q}_{jp})^{\mathrm{T}}(\mathbf{I} + \mathbf{H}_j)\Big] \boldsymbol{c}_j = \mathbf{T}_p \boldsymbol{d}_p^{\mathrm{I}} \ , \ p = 1, \ldots, N \ . \tag{2}$$

Here, δ_{jp} is the Kronecker delta, $\mathbf{I}$ is the identity matrix, and $(\cdot)^{\mathrm{T}}$ denotes a matrix transpose. The radiation transfer matrix $\mathbf{H}_j = -\mathrm{i}\omega \boldsymbol{\varrho}_j \mathbf{A}_j^{-1} \hat{\mathbf{F}}_j^{\mathrm{T}}$ relates the scattered wave amplitudes to the amplitudes of radiated waves (unit-velocity radiated wave matrix $\boldsymbol{\varrho}_j$; body dynamics matrix $\mathbf{A}_j$, diffraction force transfer matrix $\hat{\mathbf{F}}_j$). The effect of array configuration is expressed through matrices $\mathbf{S}_{jp}$ and $\mathbf{Q}_{jp}$. The separation matrix $\mathbf{S}_{jp}$ depends only on the relative positions of the bodies in the array; the periodicity matrix $\mathbf{Q}_{jp}$ encodes the effect of the periodically repeated bodies [3]. In order to solve (2), we limit the maximum order of partial waves to N_{p} and truncate the number of evanescent waves to M. Except for the error introduced by the truncation, the solution to the system (2) is, in principle, exact. The complex motion amplitude $\boldsymbol{X}_j$ can then be evaluated through the body equation of motion as $\boldsymbol{X}_j = \mathbf{A}_j^{-1} \hat{\mathbf{F}}_j^{\mathrm{T}} \boldsymbol{c}_j$.

The free surface, far away from a periodic array, can be expressed purely in terms of outward-propagating scattered plane waves (or modes). The transmitted modes (complex amplitude A_m^{+}) propagate at angle θ_m, while the reflected modes (complex amplitude A_m^{-}) propagate at angle $\pi - \theta_m$. The propagation angle θ_m is determined from the diffraction grating equation $\sin\theta_m = \sin\theta_{\mathrm{I}} + m\,2\pi/kd$, $m \in \mathbb{Z}$. For an array with periodicity d, the critical wavenumbers $(kd)_m^{\mathrm{cr}}$ at which new mode appear (known as Rayleigh wavenumbers) are given by $|\sin\theta_{\mathrm{I}} + 2\pi m/(kd)_m^{\mathrm{cr}}| = 1$. As the energy at $(kd)_m^{\mathrm{cr}}$ is abruptly redistributed among the scattered modes, resulting in an abrupt change in the behaviour of bodies in the array, we refer to these instances as Rayleigh resonances [3].

Multiple scattering model for C-W arrays

To calculate the response of an array in front of an infinite vertical wall, we employ the method of images. Let the vertical wall be located at the $x = 0$ plane; the mirror images of bodies $\mathcal{B}_p(x_p, y_p)$, $x_p < 0$, are then $\mathcal{B}_{p'}(-x_p, y_p)$, figure 1b. A solution is calculated for the expanded array of $2N$ bodies (both $\mathcal{B}_p$ and $\mathcal{B}_{p'}$ included) for an incident wave in θ_{I} direction. The no-flux boundary condition $\partial\phi/\partial x = 0$ on the wall can be satisfied by superposing a solution for a mirrored incident wave from $\theta_{\mathrm{I}}' = \pi - \theta_{\mathrm{I}}$ direction on the same expanded array. The superposed $\theta_{\mathrm{I}} + \theta_{\mathrm{I}}'$ solution automatically satisfies all the other boundary conditions (body radiation and diffraction) due to linearity.

The solution for the θ_{I}'-direction does not need to be separately calculated as it is contained in the solution for the θ_{I}-direction on the expanded array. The amplitudes of the partial incident wave at $\mathcal{B}_j$ are $d_{m,n}^{\mathrm{I},j}(\theta_{\mathrm{I}}') = (-1)^n \exp\left[-\mathrm{i}kR_j\cos(\theta_{\mathrm{I}}+\alpha_j) + \mathrm{i}n\theta_{\mathrm{I}}\right]$, which can be expressed in terms of amplitude on body $\mathcal{B}_{j'}$ for the incident wave in θ_{I} direction (noting that $\alpha_j = \pi - \alpha_{j'}$). Hence, the solution for the scattered wave amplitudes $c_{m,n}^{j}$ for the mirrored incident wave θ_{I}' on the body $\mathcal{B}_j$ can be related to those for the incident wave in θ_{I} direction through $c_{m,n}^{j}(\theta_{\mathrm{I}}') = c_{m,-n}^{j'}(\theta_{\mathrm{I}})$, i.e. $c_{m,n}^{j}(\theta_{\mathrm{I}}')$ are equal to the scattered waves amplitudes of the mirrored body of the opposite sign order. For a vector of scattered wave coefficients $\boldsymbol{c}_j$ on body $\mathcal{B}_j$, we employ the notation $\tilde{\boldsymbol{c}}_j$ when the partial waves are in the reverse order. The total scattered wave amplitude vector $\boldsymbol{c}_j^{\mathrm{W}}$ for a body $\mathcal{B}_j$ in front of a wall is $\boldsymbol{c}_j^{\mathrm{W}}(\theta_{\mathrm{I}}) \equiv \boldsymbol{c}_j(\theta_{\mathrm{I}}) + \boldsymbol{c}_j(\theta_{\mathrm{I}}')$. This can be expressed through θ_{I}-direction solutions only as $\boldsymbol{c}_j^{\mathrm{W}}(\theta_{\mathrm{I}}) = \boldsymbol{c}_j(\theta_{\mathrm{I}}) + \tilde{\boldsymbol{c}}_{j'}(\theta_{\mathrm{I}})$.

The power extracted by a body $\mathcal{B}_j$ in the array can be expressed as $P_j = {}^1\!/_2\beta\omega^2|\boldsymbol{X}_j|^2 = \boldsymbol{c}_j{}^+\boldsymbol{\Omega}_j\boldsymbol{c}_j$, where $\boldsymbol{\Omega}_j$ is the PTO-dependent, real symmetric power transfer matrix $\boldsymbol{\Omega}_j = {}^1\!/_2\beta\omega^2\hat{\mathbf{F}}_j(\mathbf{A}_j^{-1})^+\mathbf{A}_j^{-1}\hat{\mathbf{F}}_j^+$ of $\mathcal{B}_j$ ($(\cdot)^+$ denotes a Hermitian transpose). The power extracted by a body $\mathcal{B}_j$ in front of a wall is then

$$P_j^{\mathrm{W}} = \left(\boldsymbol{c}_j^{\mathrm{W}}\right)^+\boldsymbol{\Omega}_j\boldsymbol{c}_j^{\mathrm{W}} = P_j + P_{j'} + 2\,\mathrm{Re}\left[\tilde{\boldsymbol{c}}_{j'}^{+}\boldsymbol{\Omega}_j\boldsymbol{c}_j\right] \,, \tag{3}$$

where all the quantities are calculated on the extended $2N$ array for the incident wave in θ_{I} direction. The total power extracted by an array in front of a wall is $P = \sum_{j=1}^{N} P_j^{\mathrm{W}}$.

Results and Discussion

We analyse the energy extraction performance of C-W arrays as a function of the periodicity d and the distance to the wall d_{w}. Due to the strong reflection from the wall, the peak gain q_{W} of a C-W array can be significantly increased when compared to a single periodic row of WECs (S-array) with identical periodicity d, figure 2a. In the long-wave $ka \to 0$ limit, $q_{\mathrm{W}} \to 4$ regarldless of the array configuration. This occurs due to the weak scattering off of the bodies and the doubling of the total wave amplitude, leading to quadrupling of the extracted power. With the wavenumber increase, the scattering is stronger and even larger gains are possible. For example, at the body resonant wavenumber k_{r}, a select configuration ($d/2a = 6$, $d_{\mathrm{w}}/2a = 3.5$) achieves a gain of $q_{\mathrm{W}}(k_{\mathrm{r}}) = 7.3$, which is significantly larger than $q_{\mathrm{S}}(k_{\mathrm{r}})$ of the S-array with the same periodicity ($q_{\mathrm{W}}/q_{\mathrm{S}} \approx 5$). The presence of the wall introduces new interferences, characterized by additional peaks and troughs in gain. As the wavenumber increases ($k > k_{\mathrm{r}}$), these peaks are getting narrower.

The contour plot of q_{W} as a function of spatial configuration (d and d_{w}) reveals the structure behind the peaks in q_{W}, plotted for k_{r} in figure 2b. In contrast to S-arrays, C-W arrays achieve maximum q_{W} values for configurations that operate above the first critical wavenumber $(kd)_1^{\mathrm{cr}}$. The high values of q_{W} are bounded by low-value regions at regular kd_{w} intervals caused by destructive interferences. Rayleigh resonances occurring at $(kd)_m^{\mathrm{cr}}$ result in lower values of q_{W}, similar to their effect on q_{S} in single-row periodic WEC arrays. At $\theta_{\mathrm{I}} = 0$, the optimal C-W configuration achieves $q_{\mathrm{W}}^* \approx 8$, which is much higher than previously reported values. For example, Konispoliatis and Mavrakos [1] find $q_{\mathrm{W}}^* \lesssim 6$ for select configurations of WEC arrays of truncated cylinders in front of a wall. In fact, we find optimal C-W configurations that achieve $q_{\mathrm{W}}^* \gtrsim 6$ for all $\theta_{\mathrm{I}} \lesssim 45°$.

The areas of high q_{W}-values achieved by many C-W configurations, figure 2c, are criss-crossed by regions where q is significantly lower. These features are due to the additional interactions that exist in multi-row periodic arrays and which can be explained by a plane-wave interaction model that neglects the near-field interactions and considers only a single scattering event between rows [4].

The interaction between the wave incident at θ_{I} and a wave reflected from a periodic structure propagating at $\pi - \theta_{\mathrm{I}}$ results in an undulating free surface envelope, with generatrix parallel to the reflecting structure. We refer to this as Bragg interference. The minima of the envelope (i.e., destructive

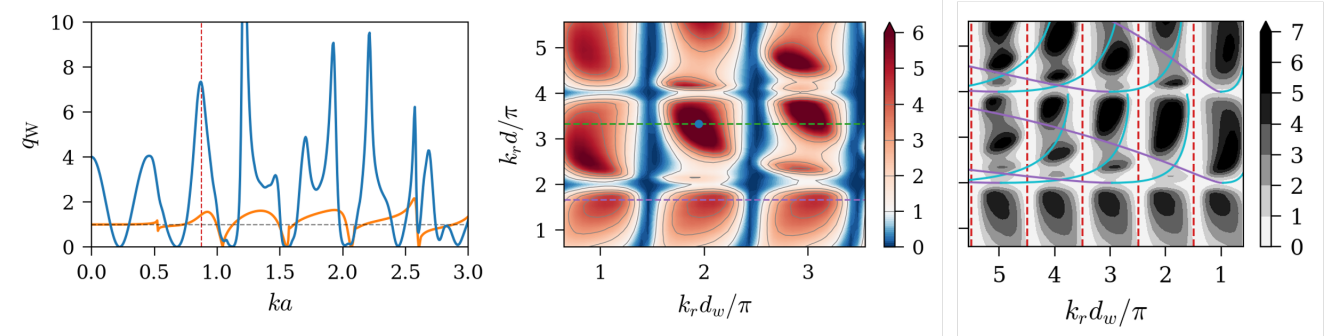

Figure 2: Performance of C-W arrays in normal incidence. (a) Comparison of array gain of a particular C-W configuration ($d/2a = 6$, $d_w/2a = 3.5$; blue line) with an equivalent S-array configuration ($d/2a = 6$, orange line) as a function of wavenumber k. (b) Contour plot of q_W as a function of array configuration (d, d_w) for the body resonant wavenumber k_r. (c) Single-scattering predictions of destructive Bragg (dashed lines) and Laue (solid lines) interferences. (Note the horizontal axis is reversed.)

Bragg interferences) are located at

$$kd_w \cos\theta_I = n\pi + \delta^B/2, \quad n \in \mathbb{Z} \tag{4}$$

where d_w is the distance from the wall, and δ^B is the phase shift of the reflected wave. This phase shift generally depends on the periodicity d; for a wall, $\delta^B = \pi$. If the row of WECs is placed at one of the minima of the wave envelope, the WEC motion is diminished, resulting in low q_W-values. Constructive Bragg interference, occurring for $\delta^B + \pi$, results in maximum q_W for a particular d.

The interaction between an incident wave and a higher scattered mode $A_m^{\pm}$, $|m| \geq 1$, the so-called Laue interference [4], leads to a similar undulating wave envelope. The minima of the envelope resulting from destructive Laue interferences between the incident wave and the m-th mode occur at

$$kd_w(\cos\theta_I - \cos\theta_m) = 2n\pi + \delta_m^L, \quad n \in \mathbb{Z}\,. \tag{5}$$

The phase shift δ_m^L of mode m depends on the array configuration and again on d. For C-W arrays, $\delta_m^L(d) = \arg(A_{m,C}^+)$, where the additional subscript to $A_m^{\pm}$ refers to the row at which the phase shift occurs. Constructive Laue interferences occur at $\delta_m^L + \pi$.

The conditions (4) and (5) translate into a family of lines in d–d_w space. The interference lines (ILs) corresponding to destructive Bragg and Laue interferences predict well the minima of gain in C-W arrays obtained through multiple-scattering simulations, figure 2c. The maxima of q contained between the drawn destructive ILs lie near the constructive ILs (not drawn). While the conditions for Bragg and Laue interferences are determined by the array configuration and the phase shift at the scattering structure, their strength is governed by the amplitudes of the interacting modes. As such, some Bragg and Laue interferences are less noticeable when the interfering scattered modes are not strong.

References

[1] D. N. Konispoliatis and S. A. Mavrakos. "Wave Power Absorption by Arrays of Wave Energy Converters in Front of a Vertical Breakwater: A Theoretical Study". *Energies* 13 (8) (2020), p. 1985.

[2] E. Loukogeorgaki et al. "Layout optimization of heaving Wave Energy Converters linear arrays in front of a vertical wall". *Renewable Energy* 179 (2021), pp. 189–203.

[3] G. Tokić and D. K. P. Yue. "Hydrodynamics of periodic wave energy converter arrays". *Journal of Fluid Mechanics* 862 (2019), pp. 34–74.

[4] G. Tokić and D. K. P. Yue. "Axisymmetric reflectors in wave energy converter arrays: Harnessing scattering to increase energy extraction". *Physics of Fluids* 35 (2023), p. 067120.